Segregation Behaviour of Third Generation Advanced High-Strength Mn-Al Steels

A. Grajcar*

Silesian University of Technology, Institute of Engineering Materials and Biomaterials,
Konarskiego 18a, 44-100 Gliwice, PL
*Corresponding author. E-mail address: adam.grajcar@polsl.pl

Abstract

The paper addresses the macro- and microsegregation of alloying elements in the new-developed Mn-Al TRIP steels, which belong to the third generation of advanced high-strength steels (AHSS) used in the automotive industry. The segregation behaviour both in the as-cast state and after hot forging was assessed in the macro scale by OES and by EDS measurements in different structural constituents. The structural investigations were carried out using light and scanning electron microscopy. A special attention was paid to the effect of Nb microaddition on the structure and the segregation of alloying elements. The tendency of Mn and Al to macrosegregation was found. It is difficult to remove in Nb-free steels. Microsegregation of Mn and Al between austenite and ferritic structural constituents can be removed.

Keywords: Macrosegregation, Microsegregation, AHSS, TRIP Steel, EDS, Microstructure, Hot Deformation, Microalloying

1. Introduction

Third generation of advanced high-strength steels (AHSS) for automotive industry contains significant amounts of high strength constituents, i.e. martensite, bainite and fine-grained ferrite [1]. Moreover, AHSS have a high fraction of austenitic phase, especially suitable to different strengthening mechanisms. Composite behaviour of multiphase structures and TRIP (Transformation Induced Plasticity) or TWIP (Twinning Induced Plasticity) effects related to retained austenite enable to obtain a beneficial balance between strength and ductile properties as well as desired technological forming – a very important feature for automotive components [1-3]. High amount of austenite in AHSS (between 20 and 35%) [2-4] can be achieved by chemical stabilization (C and Mn) or mechanical stabilization related to grain size refinement, e.g. using thermomechanical processing or reverse $\alpha' \rightarrow \gamma$ transformation during continuous annealing of cold rolled sheets [1, 4 and 5]. There is a trend to decrease C content below 0.2% for reasons of weldability. Recently developed steels contain increased Mn content for austenite stabilization [2-5].

TRIP steels contain also Si and Al for hampering of carbide precipitation and more recently Mo addition and Nb, Ti or V microadditions are used for further strength improvement [3-6]. Unfortunately, Mn alloying results in some problems, e.g. ability to microsegregation, localized deformation and hot-working [3-7]. A banded microstructure of ferrite / bainite-martensite-austenite is typical for TRIP steels [6 and 7]. The metallurgical reason for banded structures is segregation of Mn and Al during continuous casting [6]. Pichler et al. [6] noticed that the most significant hard bainite-martensite-austenite bands are occurred in the centre of the strips. Severe plastic deformation can lead to some damaged zones in these bands. Wietbrock et al. [7] reported that local differences in Mn content between dendrites and interdentritic spaces in high-Mn alloys (over 20 wt.%) can reach up to 7 wt.%. After some homogenization strategies the microsegregation of Mn can be much reduced. In the previous works, Grajcar et al. [8 and 9] investigated the new-developed 0.17C-(3-5)Mn-1.6Al-0.2Si-0.2Mo alloys in the as-cast state. This paper addresses the problems of macro- and microsegregation of Mn and Al after hot deformation.

2. Experimental procedure

The paper compares macro- and microsegregation of Mn and Al and the microstructures in the as-cast state and after hot-working of four new-developed high-Mn high-Al TRIP steels with and without Nb microaddition. The chemical composition given in Table 1 was designed from the point of view of maximization of retained austenite (increased Mn content) and obtaining carbide-free bainite by low-Si high-Al concept (susceptibility to galvanizing) [10]. Mo and Nb were used to enhance strength. Special attention was paid to the effect of Nb microaddition on the macro- and microsegregation behaviour as well as grain refinement.

Table 1.
Chemical composition of the investigated steels (mass content, %)

	C	Mn	Al	Si	Mo	Nb	S	P
3MnAl	0.17	3.3	1.7	0.22	0.23	-	0.014	0.010
3MnAlNb	0.17	3.1	1.6	0.22	0.22	0.04	0.005	0.008
5MnAl	0.16	4.7	1.6	0.20	0.20	-	0.004	0.008
5MnAlNb	0.17	5.0	1.5	0.21	0.20	0.03	0.005	0.008

Steels were produced by vacuum induction melting in the Balzers VSG-50 furnace at the Institute for ferrous Metallurgy in Gliwice. Liquid metal was cast in the Ar atmosphere into a hot-topped closed-bottom wide-end-up cast iron mould with internal dimensions: bottom – $\varnothing$ 122 mm, top – $\varnothing$ 145 mm, height – 200 mm (without ingot head). To evaluate the susceptibility of alloys to macrosegregation the ingots were cut perpendicular to an axis of the ingot within the distance of 30 mm from the bottom. The chemical composition along a diameter was tested in the macro scale by optical emission spectroscopy (OES). Measurements were carried out in a central zone, within the distance of about 31 mm from the middle and in an external zone of ingots.

The microsegregation in different regions of nital-etched as-cast specimens was examined by energy dispersive spectrometry (EDS). Comparable linear analyses as well as point analyses of different structural constituents were carried out using EDAX in the SUPRA 25 scanning electron microscope (SEM).

Successively, the ingots with a mass of 25 kg after austenitizing at 1200°C for 3 hours were forged at a temperature range from 1200 to 900°C to a final width of 160 mm and a thickness of about 22 mm. To compare the microstructures in the as-cast state and after hot forging metallographic investigations were carried out by the use of LEICA MEF4A microscope. The specimens after hot forging were cut near the edge of a flat according to its length. The microstructure of the plastically deformed specimens was revealed by etching in 10% aqueous solution of sodium metabisulfite for better identification of retained austenite. EDS measurements were carried out to assess the differences in chemical composition between surface (about 2 mm below surface) and central regions of a plastically deformed flat. Moreover, the local microanalysis of chemical composition by EDS in different micro-constituents of hot-forged specimens was performed.

3. Results

To compare the chemical composition in different zones of the ingots according to the nominal composition (Table 1), comparable schemes of the distribution of individual elements along a diameter are shown in Fig. 1a-c.
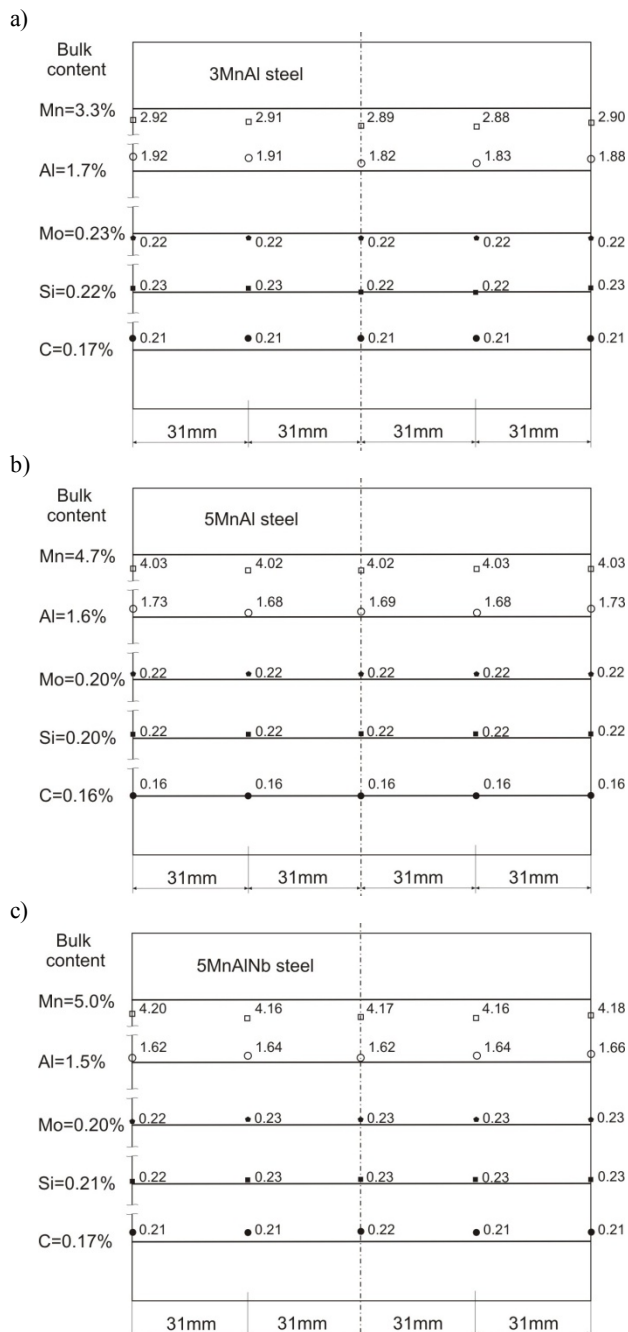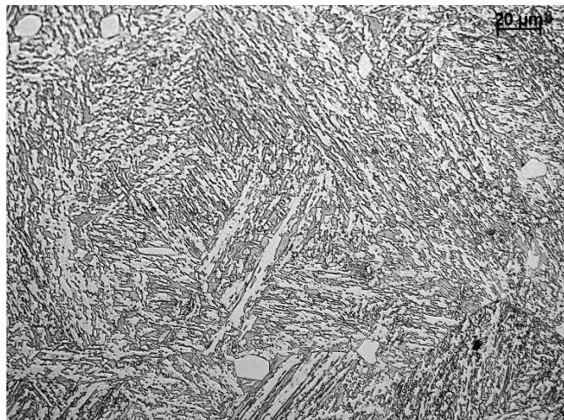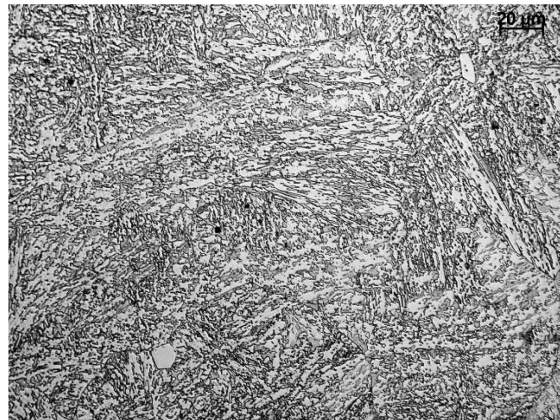
a)

b)

c)

Fig. 1. Chemical composition measured by OES at the transverse sections of the 3MnAl (a), 5MnAl (b) and 5MnAlNb ingots (c)
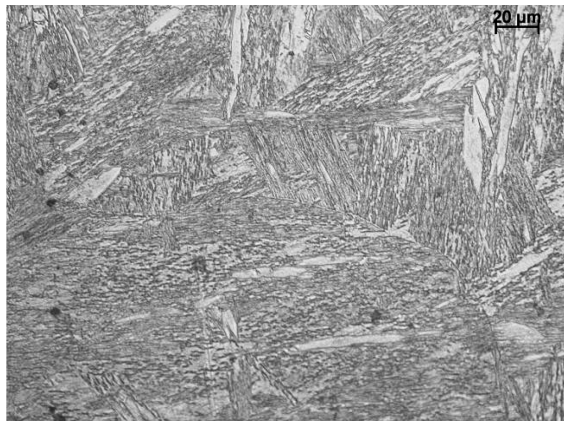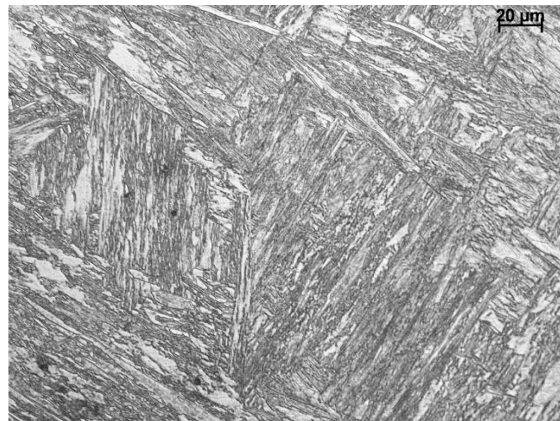
a) 3MnAl

b) 3MnAlNb

c) 5MnAl

d) 5MnAlNb

Fig. 2. Primary microstructures revealed at transverse sections of the 3MnAl (a), 3MnAlNb (b), 5MnAl (c) and 5MnAlNb (d) ingots

Results in Fig. 1 indicate the good homogeneity of chemical composition in different zones of a transverse section of the ingots. Mo and Si contents are the same like the bulk content for 3MnAl steels (Fig. 1a), whereas for 5MnAl steels they are slightly higher (Fig. 1b-c). Their concentrations are stable along a diameter of the ingots. It is characteristic that C and Al contents are higher compared to the bulk composition (except C for the 5MnAl steel). The carbon content near the bottom of the ingot is consistent with the nominal composition only for 5MnAl steel (Fig. 1b). However, segregation of carbon in the as-cast samples should not be a problem considering successive hot-working and a high diffusion rate of interstitial elements at high temperatures.

The most interesting results concerning segregation in the as-cast state were observed for Mn and Al. The highest difference in alloying element concentration was observed for Mn. Manganese contents are nearly the same along a diameter but much lower compared to the bulk content (Table 1). The difference is about 0.4 wt.% for the 3MnAl steels and twice higher for steels containing higher Mn content. The most significant difference of chemical composition in different zones of the ingot can be noticed for Al. Its content decreases from external to center zones of the ingots (Fig. 1a-b). The concentration gradient is relatively small because the maximum difference in Al content between the

external and centre zones does not exceed 0.08%. The effect is more visible for the steels without Nb (Fig. 1a-b). The change of Al along a diameter is according with the thermodynamic calculations performed by Pichler et al. [6].

Figure 2 reveals primary microstructures of the ingots. In the previous works [8 and 9], it was demonstrated that in an external region of the ingots columnar-like crystals can be observed whereas the majority of the ingots consists of chaotically arranged dendrites. At higher magnifications some morphological details of the as-cast microstructures can be seen. In all the steels a growth of austenite transformation products began at primary boundaries of γ phase. Each primary austenite grain contains a few colonies of a lath morphology. Bainite is a main structural constituent of steels containing 3% Mn (Figs 2a-b). Several ferrite grains located along primary austenite boundaries can be also found. Steels containing a higher Mn concentration have higher hardenability what results in the clear lath microstructure of bainite and martensite (Fig. 2c-d). No distinct effect of Nb microaddition on grain refinement for as-cast specimens was observed.
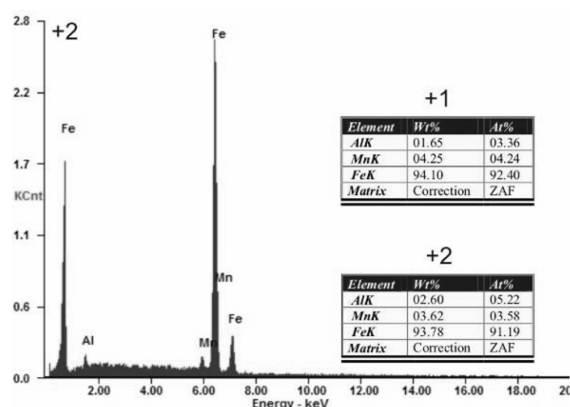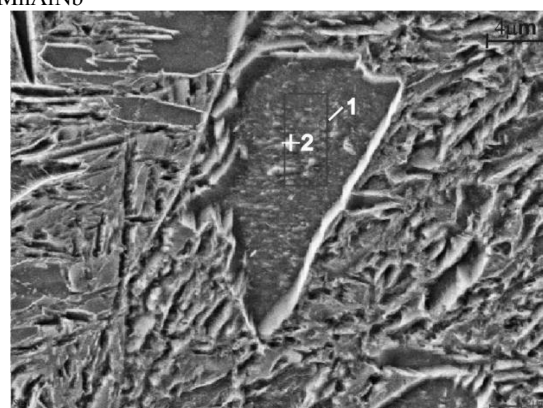
a) 3MnAlNb
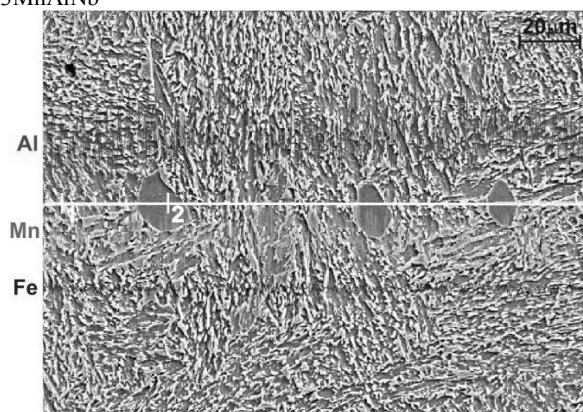
b)

Fig. 3. Bainitic-martensitic-austenitic microstructure of the 3MnAlNb steel containing a few ferrite grains and linear distribution of Al, Mn and Fe concentration along the white line (a) and EDS spectrum from the point 2 in Fig. a (b)

The microstructure in Fig. 3a reveals that 3MnAl steels also contain some retained austenite. This phase occurs in boundary regions of ferrite grains due to carbon escape during the $\gamma \rightarrow \alpha$ transformation. Additionally, the γ phase is located between individual laths of bainite. In 5MnAl steels a majority of retained austenite is of an interlath type (Fig. 4a). The occurrence of austenitic phase confirmed also by X-ray but those results will be reported elsewhere.

Linear comparable analysis of the Mn and Al distribution across the bainitic and martensitic laths did not revealed significant changes for 5MnAl steels. The similar situation takes place for 3MnAl steels except the difference between ferrite grains and the rest of structural constituents. It can be observed that ferrite grains usually contain higher Al and lower Mn concentration (Fig. 3a), what is reasonable taking into account the austenitic and ferritic nature of Mn and Al, correspondingly. The situation in bainitic-martensitic-austenitic regions is opposite. The examples of the EDS analysis in the points 1 and 2 (Fig. 3a) are given in Fig. 3b.
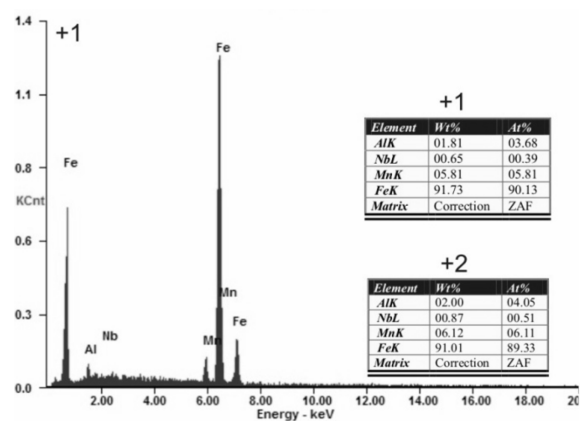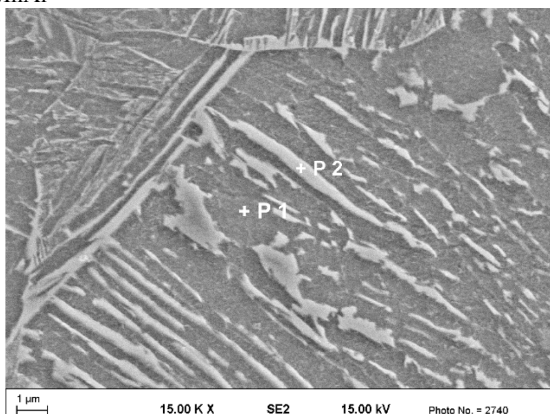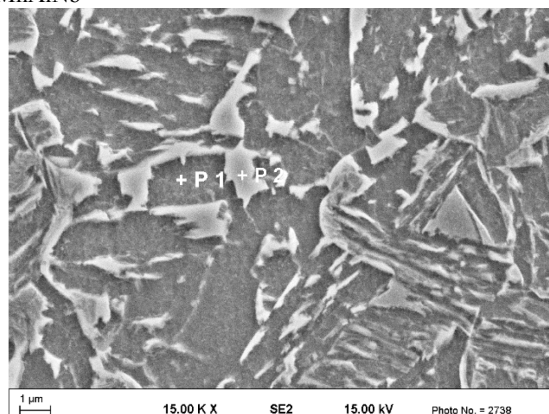
a) 5MnAlNb

b)

Fig. 4. Intra-lath particles as the example of the degenerate lower bainite structure in a bainitic-martensitic-austenitic matrix of the 5MnAlNb steel (a) and EDS spectrum from the region 1 in Fig. a (b)

An interesting morphological feature of steels containing 5% Mn is a structural constituent inside large bright laths (Fig. 2c-d). Its morphology is better visible in SEM (Fig. 4a). These are fine particles inside bainitic ferrite. It is interesting that the EDS spectrum (Fig. 4b) from the region 1 in Fig. 4a did not revealed the increase of any alloying element, i.e. C, Nb, Al, N, Mn, Mo (with the exception of slightly increased Mn, Al and Nb contents measured during the whole EDS investigation). The same result was obtained when focusing on the particle in the point 2 (Fig. 4a-b). In this way, the possibilities of the occurrence of Nb(C,N) or AlN were excluded. It is also confirmed by the presence of these particles in the steel without Nb. Precipitation of AlN is low probable when taking into account a low concentration of N in all the steels (below 50 ppm). The obtained structure in Fig. 4a is similar to that discovered by Zajac et al. [11], which classified new bainitic microstructures - beyond classification based on conventional concepts. The structure in Fig. 4a is most similar to degenerate lower bainite. It consists of very fine, fragmented martensite/austenite (MA) particles inside bainitic ferrite laths.
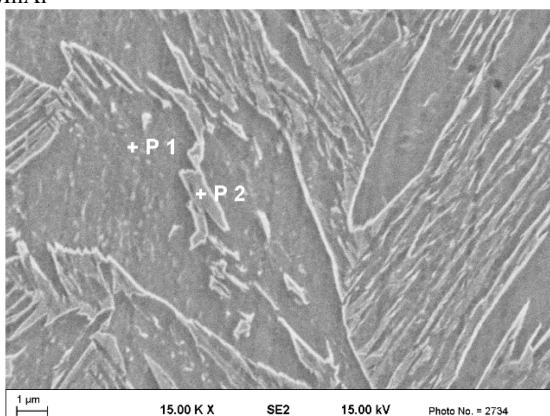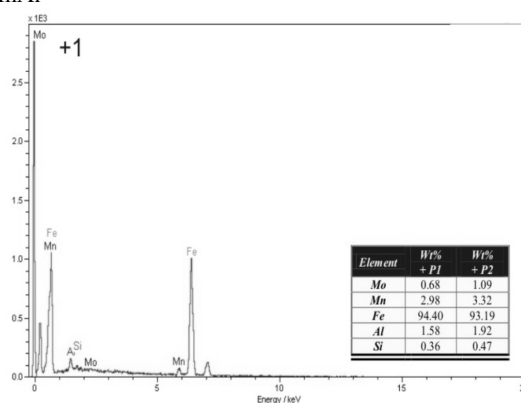
a) 3MnAl

b) 3MnAlNb

c) 5MnAl

d) 3MnAl

Fig. 5. Bainitic-martensitic-austenitic microstructures of the 3MnAl (a), 3MnAlNb (b), 5MnAl (c) steels after hot deformation
and EDS spectrum of the 3MnAl steel from the point 1 in Fig. a (d)

Hot deformation is a reason of the significant refinement of all the microstructures (Fig. 5). It concerns both the primary austenite grains and bainitic-martensitic regions. The fractions of retained austenite are higher when comparing to the as-cast state (Figs 2, 3). It is due to deformation-induced enrichment of the γ phase in carbon. The fraction of retained austenite is comparable in 3MnAl steels (Fig. 5a-b) and higher comparing to 5MnAl steels (Fig. 5c). The interlath austenite of various thickness is usually stable (Fig. 5a) whereas the blocky-type austenite transformed partially to martensite during cooling (Fig. 5b). The brightest regions in the microstructure of the 5MnAl steel indicate that retained austenite is located only at the boundaries of granular bainitic ferrite and as films between individual laths of bainitic ferrite or bainitic ferrite and martensite (Fig. 5c). The martensite/austenite particles inside granular bainitic ferrite are also present for the plastically deformed specimens.

The microstructures are quite homogeneous what indicates that austenitizing of the ingots at 1200°C for 3 hours followed by hot forging is sufficient to remove local microsegregation of Al and Mn. It is confirmed by EDS analyses of the chemical composition of different structural constituents (points 1 and 2 in Fig. 5a-c). The example of EDS spectrum in Fig. 5d reveals a lack of the distinct difference in Al and Mn content between retained austenite and bainitic ferrite. It is true for all the investigated steels. Despite the lack of the microsegregation of alloying elements the EDS data given in Table 2 indicate that the ability to macrosegregation between the middle and external parts of the plastically deformed flats still exists. It can be seen that the 3MnAl and 5MnAl steels have higher content of Al and lower content of Mn in the external part of the flat compared to its middle region. The same situation has taken place for the as-cast specimens (Fig. 1). However, it is interesting that it is not true for the Nb-microalloyed steels (Table 2), where the contents of Mn and Al are nearly the same at the whole thickness of the flats.

Table 2.
EDS measurements of the Mn and Al content in the centre and external parts of the plastically deformed flats (wt. %)

Grade	Mn		Al	
	centre	external	centre	external
3MnAl	3.26	2.59	1.34	2.27
3MnAlNb	3.17	3.09	1.01	0.96
5MnAl	6.03	5.12	1.16	1.33
5MnAlNb	5.25	5.42	1.55	1.81

4. Discussion

The results of the macrosegregation of alloying elements at the cross section of the as-cast ingots revealed the tendency of Mn, Al and C to segregation between the centre and external regions of the ingots (Fig. 1). C and Al contents are higher compared to the bulk composition. Taking into account that cooling conditions at the bottom are comparable to these along a perimeter of the ingots and the overall balance of chemical composition in the alloys, it is anticipated that the contents of C and Al should be smaller in the middle of the ingots. As for the lower Mn content compared to the bulk content, it can be expected that its concentration should be higher at the centre (unfortunately, the investigations were carried out only near the bottom of the ingots). The decreasing concentration of Al from the external to middle region of the ingots (Fig. 1) is according with the thermodynamic calculations performed by Pichler et al. [6]. They reported that the first formed solid phases should contain more Al than the nominal composition and hence Al is depleted in the liquid phase. The opposite is true for Mn. With advancing solidification the concentration of Mn increases whereas the Al content decreases. Due to the enrichment of Mn and depletion of Al in the centre zone of the ingots, the austenite stabilization is expected there [6]. Due to a short distance of the OES measurements from the bottom the observed changes in Al content are relatively small. After plastic deformation the tendency to macrosegregation of Al and Mn in the different regions of the flats remains for the steels without Nb (Table 2). As expected, the content of Mn is higher whereas the concentration of Al is lower in the centre of the flats. However, no banding due to the delayed kinetics of ferritic transformation was observed. It is also related to high hardenability of the steels and a very small fraction of polygonal ferrite (Fig. 3a). A lack of the macrosegregation for Nb-microalloyed steels is very beneficial but requires a more detailed investigations. The most probable reason for the reduction of macrosegregation of Mn and Al between the middle and external parts of the flats is the overall refinement of the microstructure and shorter diffusion paths of all the alloying elements under conditions of hot working.

A very positive feature of all the microstructures is the presence of retained austenite of the interlath or blocky morphology (Figs 4, 5). It should be noted that this phase occurs already for air cooled specimens, without a special heat treatment used for TRIP steels. It can be expected that under conditions of C redistribution, a retained austenite fraction should be much higher. The local microsegregation of Mn and Al between ferritic and austenitic phases in the as-cast specimens (Fig. 3) was removed after applying plastic deformation (Fig. 5). The overall grain refinement due to plastic working concerns also fine particles inside bainitic ferrite identified in steels with higher Mn content (Fig. 4, 5c). These structures are similar to degenerate lower bainite [11]. The presence of intra-lath martensite/austenite particles suggests that the degenerate lower bainite is a product of incomplete transformation of austenite which inhibits the formation of cementite inside ferrite laths. Formation of degenerate lower bainite and inhibited Fe_3C formation is connected with Al, Si, Mn and Mo alloying and cooling rate at which the transformation products are formed. This problem is more detailed explained in [11].

5. Conclusions

Manufacturing processes of third generation AHSS containing increased content of alloying elements should give consideration to the tendency of Mn and Al to macrosegregation. It can be reduced by Nb microalloying due to overall grain refinement. Local segregation of Mn and Al between austenite and ferritic phases can be removed using conventional hot-working strategies.

Acknowledgements

References

[1] De Moor E., Gibbs P.J., Speer J.G., Matlock D.K. (2010). Strategies for third-generation advanced high-strength steel development. *Iron and Steel Technology. 7/11*, 133-144.

[2] Merwin M.J. (2008). Microstructure and properties of cold rolled and annealed low-carbon manganese TRIP steels. *Iron and Steel Technology. 5/10*, 66-84.

[3] Kim S.J. (2010). Effects of manganese content and heat treatment condition on mechanical properties and microstructure of fine-grained low-carbon TRIP-aided steels. *Materials Science Forum. 638-642*, 3313-3318.

[4] De Cooman B.C., Lee S., Kumar S.S (2010). Ultra-fine grained manganese TRIP steel. Proc. of 2nd Inter. Conf. "Super-High Strength Steels", Peschiera del Garda, 1-11 (CD-ROM).

[5] Grajcar A., Kuziak R. (2011). Softening kinetics in Nb-microalloyed TRIP steels with increased Mn content. *Advanced Materials Research. 314-316*, 119-122.

[6] Pichler A., Traint S., Hebesberger T.,. Stiaszny P, Werner E.A. (2007). Processing of thin multiphase steel grades. *Steel Research International. 78*, 216-223.

[7] Wietbrock B.,. Bambach M, Seuren S.,. Hirt G. (2010). Homogenization strategy and material characterization of high-manganese TRIP and TWIP steels. *Materials Science Forum. 638-642*, 3134-3139.

[8] Grajcar A., Kalinowska-Ozgowicz E., Opiela M., Lesz S. (2011). Microstructural characterization of novel increased-manganese content TRIP steels. Proc. of the 20th Inter. Conf. "METAL'2011", Brno. 1-6 (CD-ROM).

[9] Grajcar A., Kalinowska-Ozgowicz E., Opiela M., Grzegorczyk B., Gołombek K. (2011). Effects of Mn and Nb on the macro- and microsegregation in high-Mn high-Al content TRIP steels. *Archives of Materials Science and Engineering. 49/1*, 5-14.

[10] Bhattacharya D. (2011). Perspectives on coated advanced high strength steels for automotive applications, Proc. of the 8th Inter. Conf. "GALVATECH'2011", Genova. 3-11.

[11] Zajac S., Schwinn V., Tacke K.H. (2005). Characterisation and quantification of complex bainitic microstructures in high and ultra-high strength linepipe steels. *Materials Science Forum. 500-501*, 387-394.